

Follow-up of fast-moving NEAs using Rotating Drift Scan CCD technique in Ukraine and China

Anton Pomazan¹, Nadiia Maigurova², Olexander Shulga², Yin-Dun Mao¹, Zheng-Hong Tang¹

¹ Shanghai Astronomical Observatory, Chinese Academy of Science

² Research Institute “Mykolaiv Astronomical Observatory”

Outlines

1. Background

- Current state of NEAs
- Difficulties of observing NEAs

2. Rotating drift-scan CCD approach

- Principle of RDS CCD technique
- Advantages of the RDS CCD technique
- Telescopes
- Observational program
- Processing

3. Astrometric results

- Obtained observational array
- Astrometric accuracy and analysis
- Orbital analysis
- Conclusions

Current state of NEAs

NEA (Near-Earth Asteroid):

perihelion distance < 1.3 au

PHA (Potentially Hazardous Asteroids):

size > 140 m,
MOID with Earth < 0.05 au

Near-Earth Asteroids

<u>Near-Earth Asteroids</u>	29708
<u>1+ KM Near-Earth Asteroids</u>	848
<u>Potentially Hazardous Asteroids</u>	2294

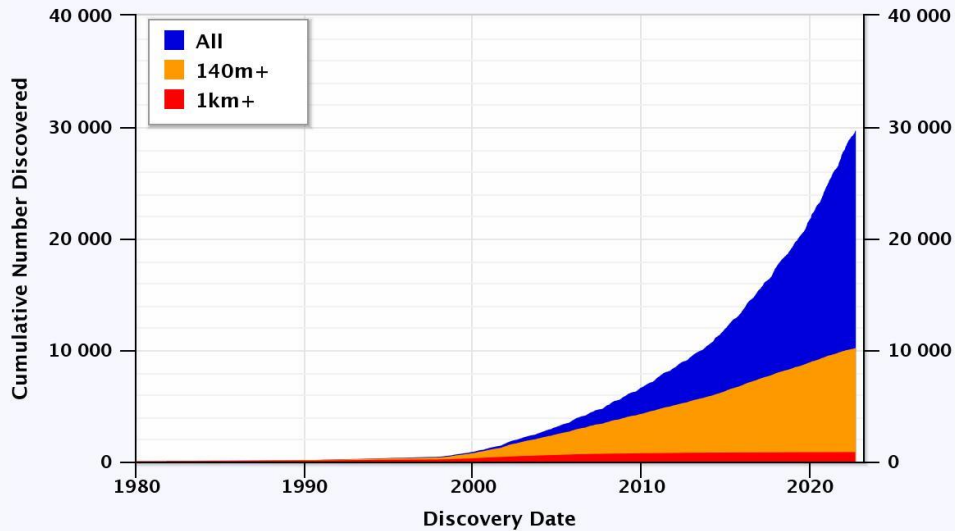
Data from IAU MPC on September 2022 <https://minorplanetcenter.net>

Current state of NEAs

Observations

Near-Earth Asteroids Discovered

Most recent discovery: 2022-Sep-17

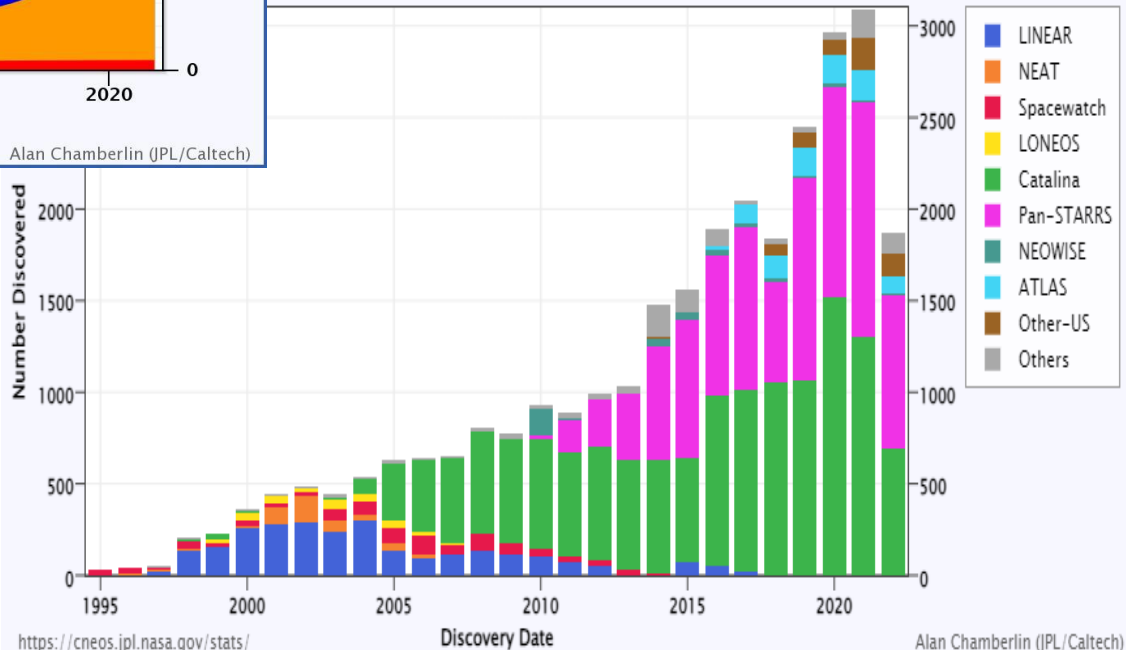


<https://cneos.jpl.nasa.gov/stats/>

Alan Chamberlin (JPL/Caltech)

Near-Earth Asteroid Discoveries by Survey

All NEAs (as of 2022-Sep-18)

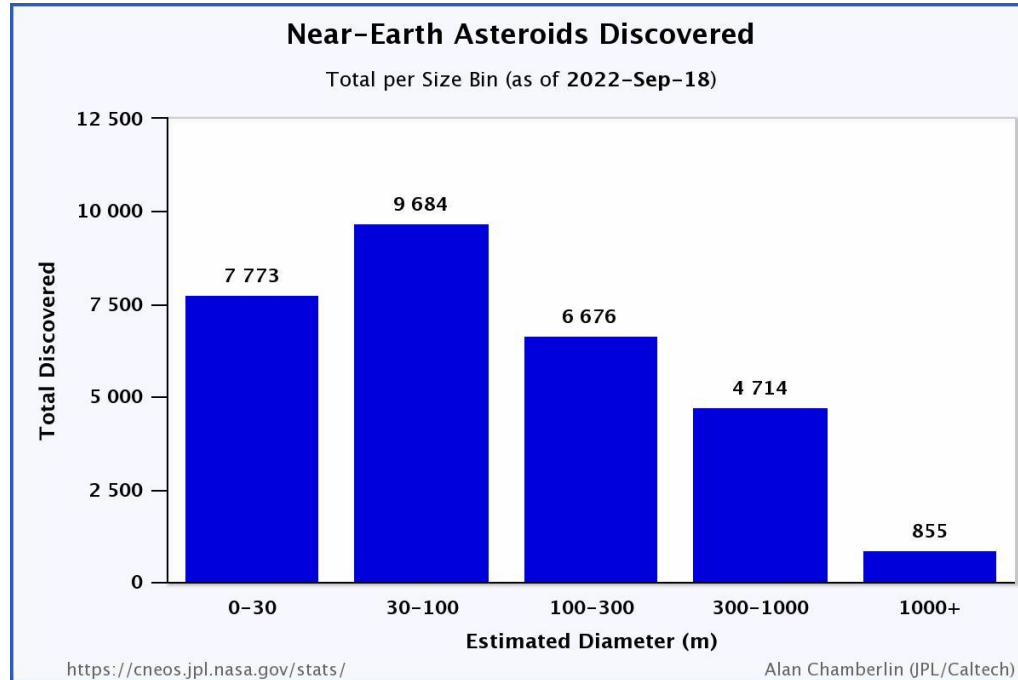


<https://cneos.jpl.nasa.gov/stats/>

Alan Chamberlin (JPL/Caltech)

Current state of NEAs

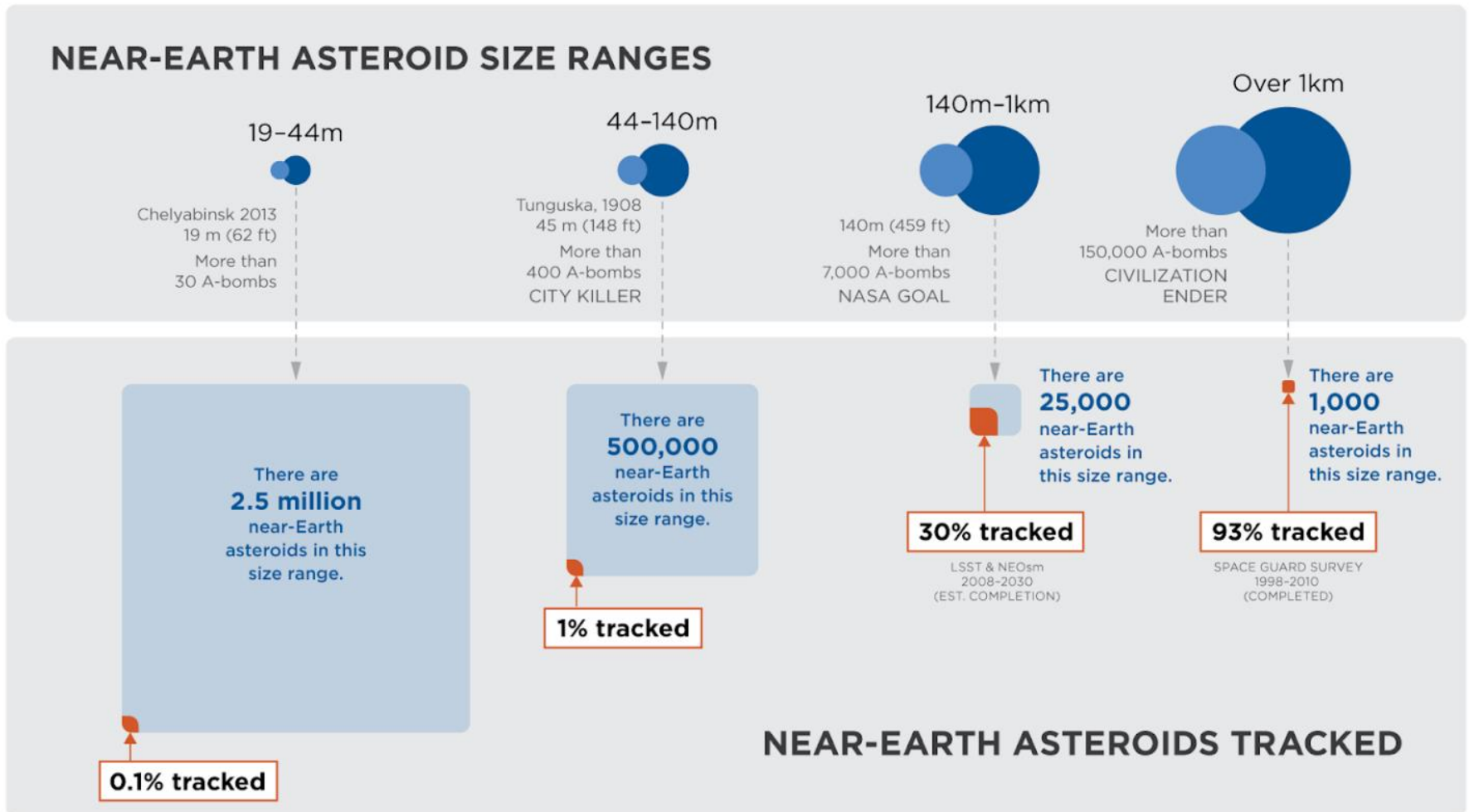
NEAs size-range distribution and completeness



Size, m	Simulation of completeness
1000+	962 ± 54 (<i>Granvik et al., 2018</i>); 940 ± 10 (<i>Harris & Chodas, 2021</i>)
100+	$(7 \pm 2) \times 10^4$ (<i>Tricarico, 2017</i>)
10+	$(1.59 \pm 0.45) \times 10^7$ (<i>Heinze et al., 2021</i>); 3.5×10^7 (<i>Trilling et al., 2017</i>)

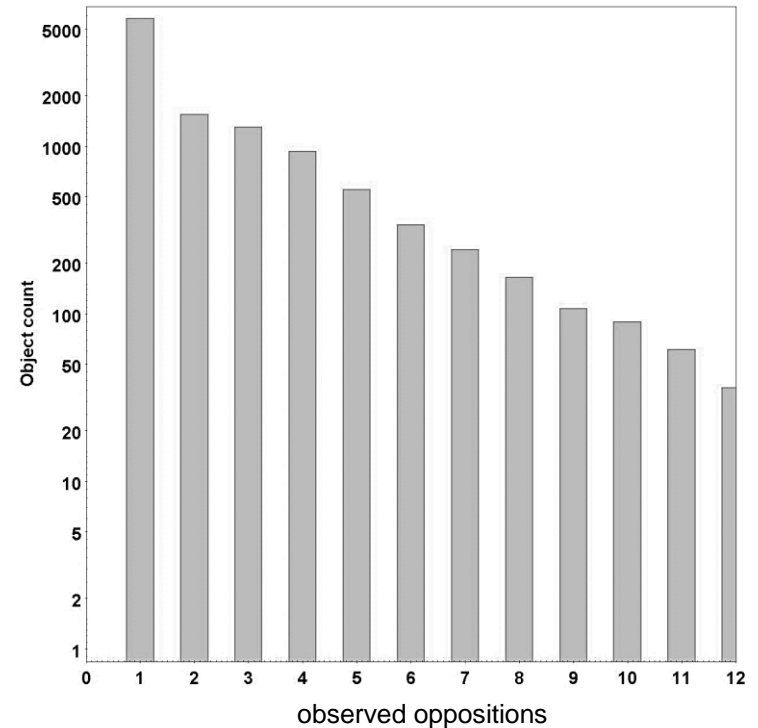
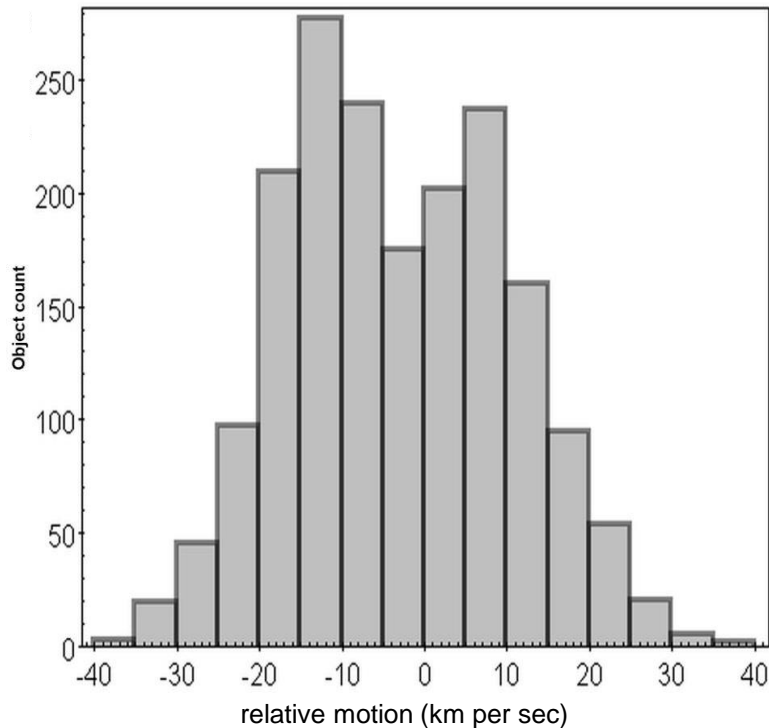
Current state of NEAs

NEAs size-range distribution and completeness (continue)



Current state of NEAs

Importance of regular follow up

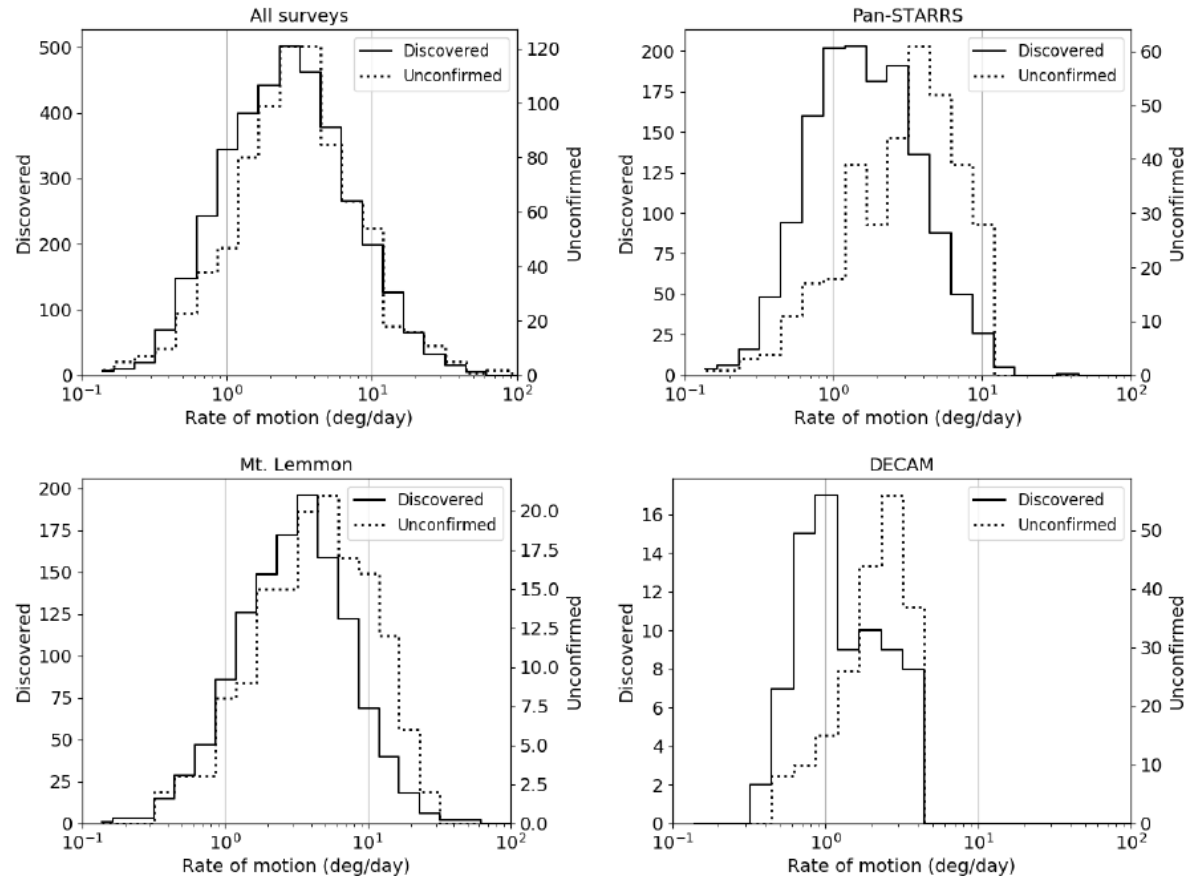


A positive "del-dot" means the NEO is moving away from the Earth, a negative "del-dot" means the NEO is moving toward the Earth. **More than 40%! of known NEO's** were discovered **after** they had approached to a minimum distance to Earth.

More than 50%! of NEAs (5755) discovered during 2000 - 2015 have been observed at **1 opposition only!**

Difficulties of observing NEAs

Apparent rate of motion. Discovery of NEAs



Reproduced from
Vereš et al., 2018, AJ, 156

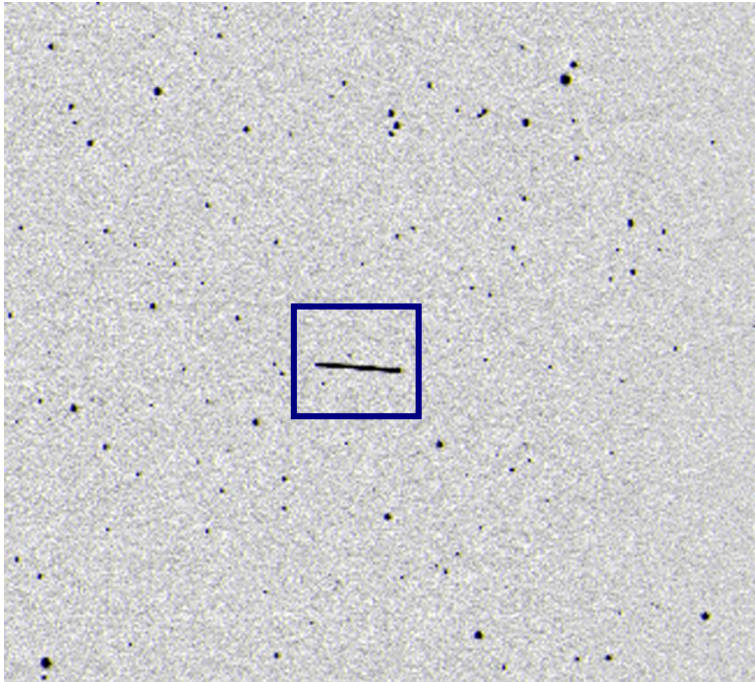
The surveys can detect fast-moving NEAs only up to a certain velocity limit, e.g. **Pan-STARRS** up to 10 deg/day (**25"/min**), DECAM3 deg/day (**7.5 "/min**).

Mt. Lemmon is able to report faster NEA candidates. This is because Mt. Lemmon has its own follow-up facilities and focuses on rapid follow-up.

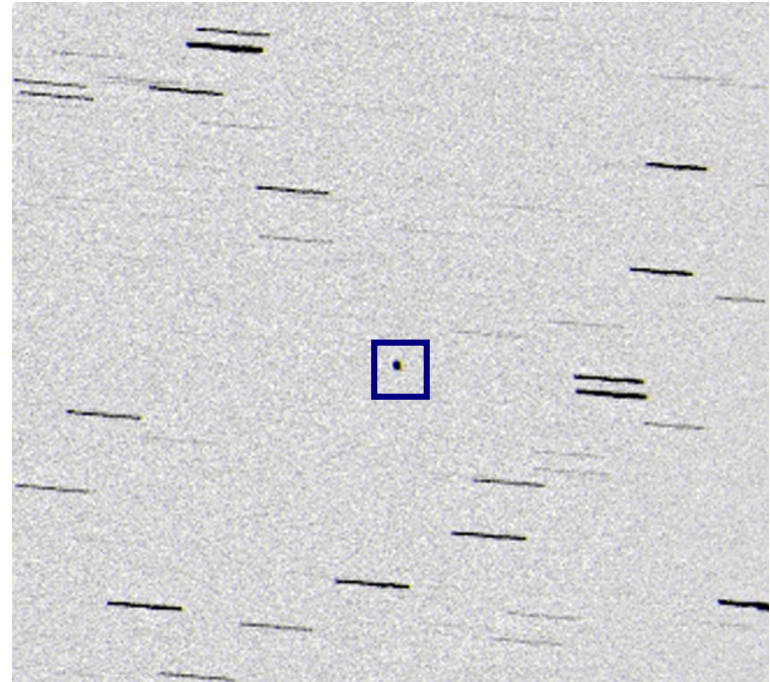
Difficulties of observing NEAs

Apparent rate of motion. Observations

Apparent motion of NEAs during CA regarding the background stars is high enough to cause trailing. It will result in streaked images and prevent to perform good astrometry for such fast moving objects.



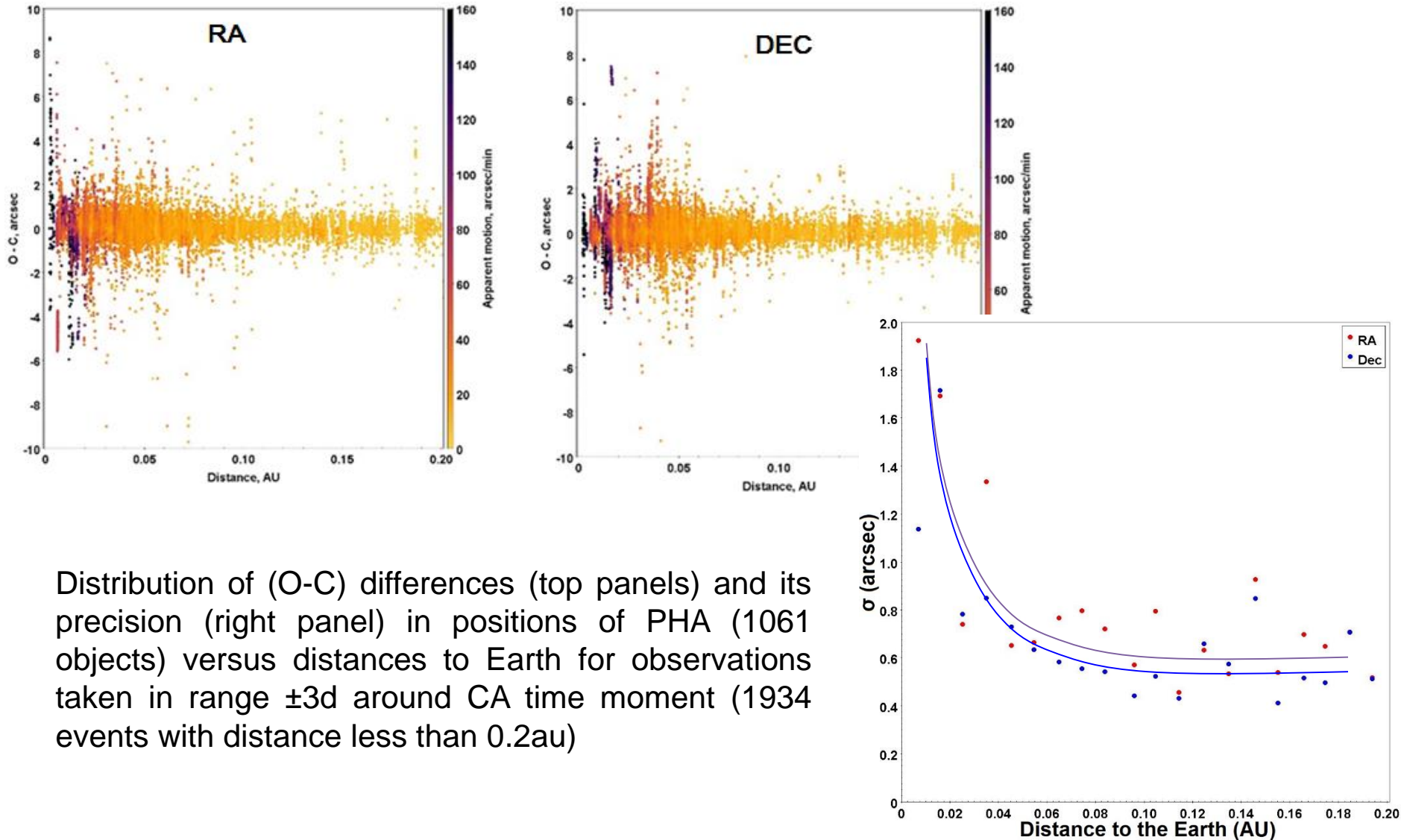
Sidereal tracking,
telescope follows stars



Object's tracking
Telescope follows NEAs

Difficulties of observing NEAs

Apparent rate of motion. Observation results



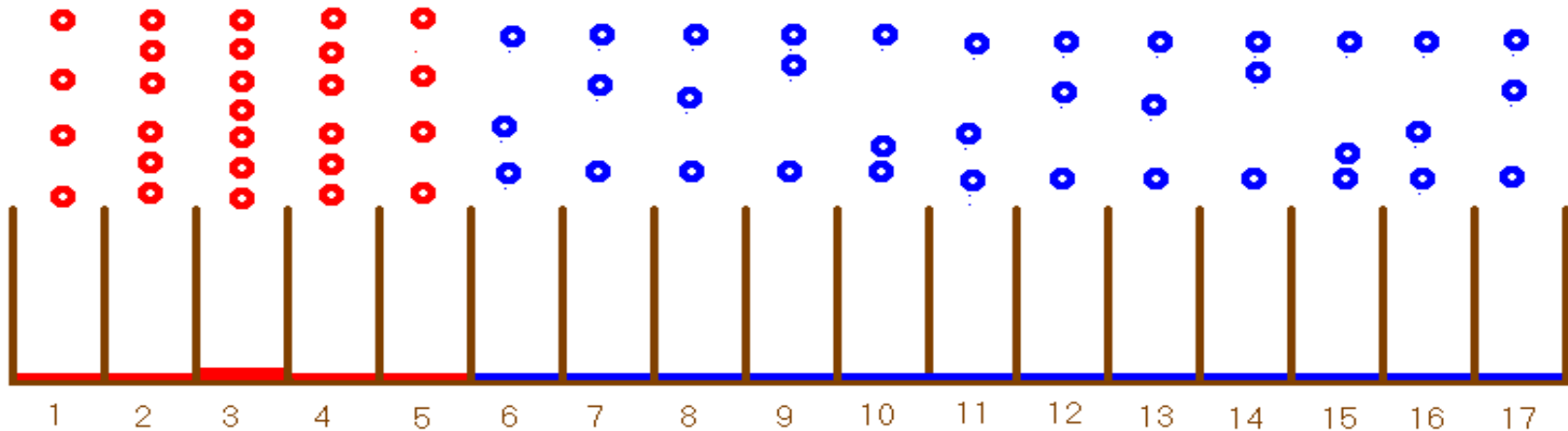
Distribution of (O-C) differences (top panels) and its precision (right panel) in positions of PHA (1061 objects) versus distances to Earth for observations taken in range $\pm 3d$ around CA time moment (1934 events with distance less than 0.2au)

Rotating drift-scan CCD approach

Original drift-scan mode

Drift-scan CCD works as:

- (1) telescope keeps pointing toward specified direction;
- (2) image of the target object moves across the CCD, charges are drifted with the relevant speed;
- (3) charges are readout during the exposing



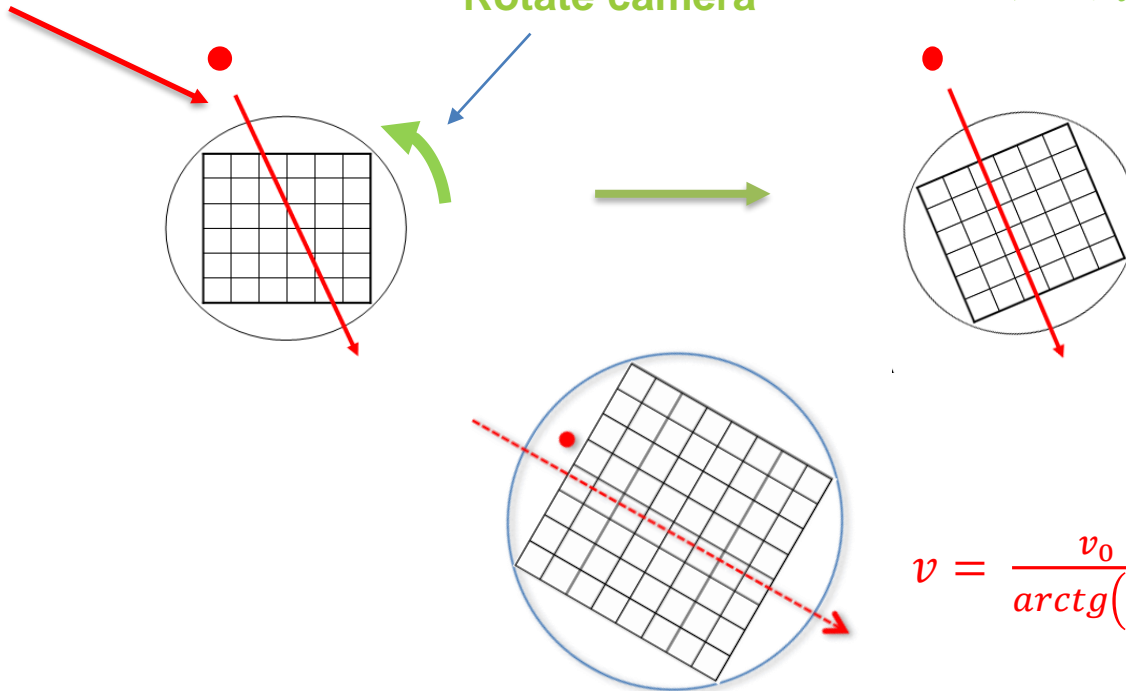
Rotating drift-scan CCD approach

RDS CCD principles

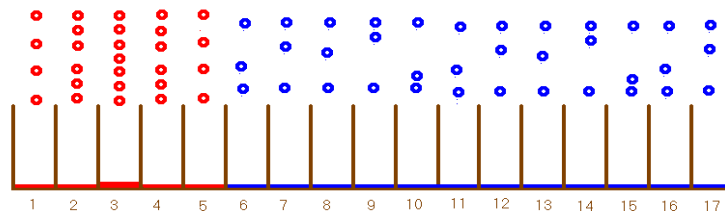
Target moving direction

Rotate camera

$$\beta = \arctg\left(\frac{v_\delta}{(v_\alpha - 15) \cdot \cos\delta}\right)$$



$$v = \frac{v_0}{\arctg\left(\frac{px}{fl}\right)}$$

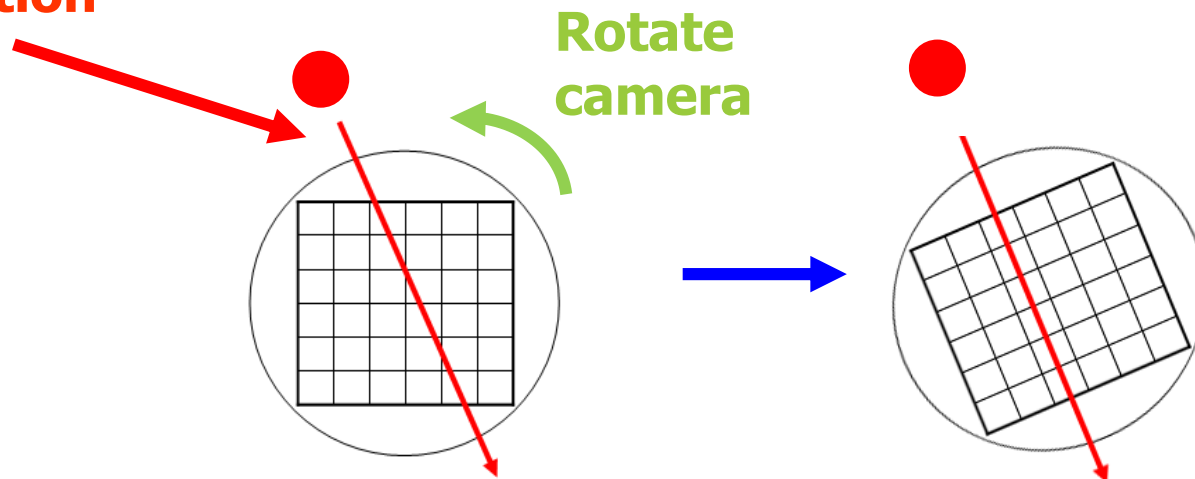


Rotating drift-scan CCD approach

RDS CCD principles

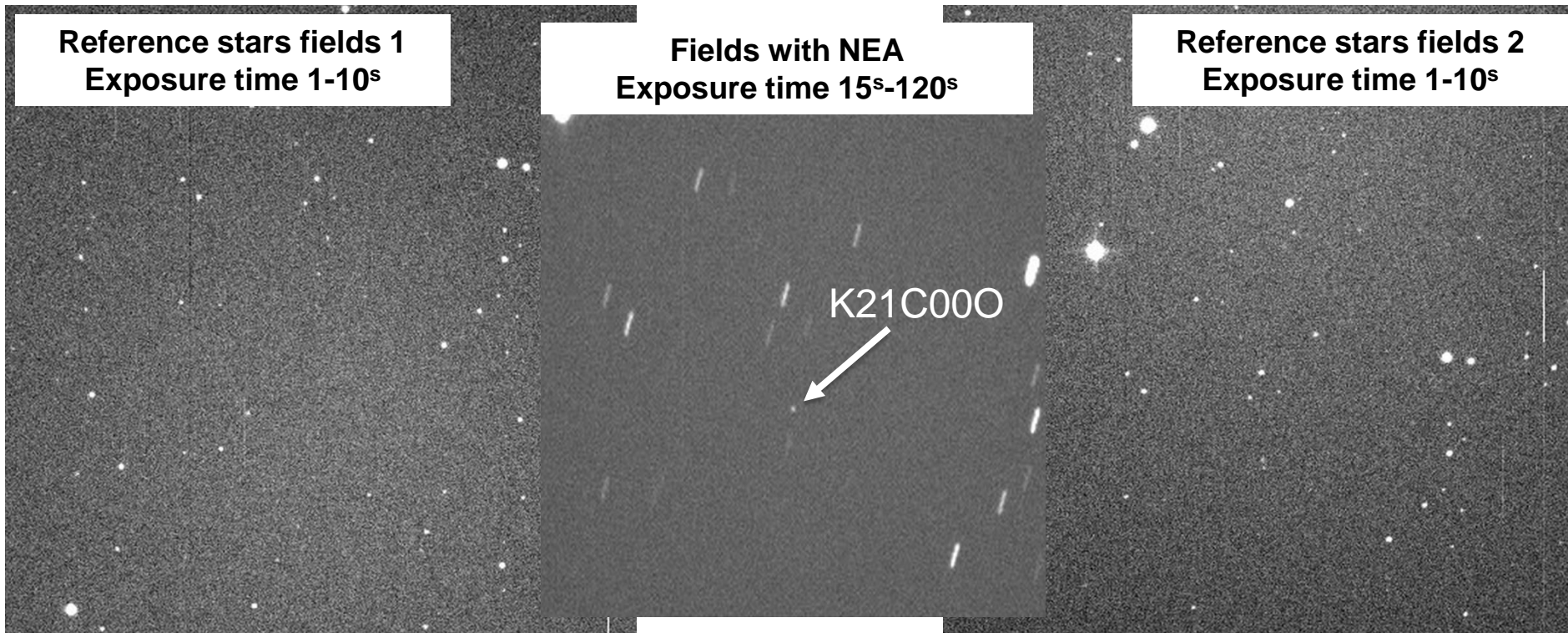
- 1) Based on prediction of the target, point the telescope toward ephemerid position;
- 2) Rotate the CCD camera to align the direction of charge transferring with direction of target object's apparent motion;
- 3) Lock the telescope and camera at the current position;
- 4) Adjust the charge transferring speed in accordance with target object's apparent motion.

Target moving direction



Rotating drift-scan CCD approach

RDS CCD observations



Three CCD frames should be taken for each RDS observation set: the first and the last frames are with background stars for reference; the middle one is with target object's point-like image. The first and the third CCD frames are used to calculate the plate model parameters for transformation between pixel coordinates and the celestial coordinates.

Rotating drift-scan CCD approach

Advantages of the RDS CCD technique

- ▶ The positions of fast-moving objects (FMO) could be as precise as for slow-moving objects, since the images of the reference stars and target objects are point-like;
- ▶ The exposure time of the object is only limited by the FOV of the telescope, so long exposures can be used for faint FMO in order to increase SNR;
- ▶ The implementation of this technique is simple and cost-effective.

References:

- Tang et al. 2014. Mem.Soc. Astron.It., 85, 821;
- Pomazan, A. et al. 2021. RAA, 21, id.175;
- Pomazan, A. et al. 2022. P&SS, 216, id.105477

Rotating drift-scan CCD approach

Processing and astrometric reductions

Logic of reductions:

Equatorial coordinates of the reference stars



Horizontal coordinates of the reference stars



Plate constants of stars' CCD frames



Linear interpolation of plate constants
to time moment of object's CCD frame



Horizontal coordinates of an object



Equatorial coordinates of an object

Developed software in ShAO:

Is written in Python (3.x) language

Uses specialized modules:
NumPy, SciPy, Astropy, PALpy

Transformation equatorial coordinate to
horizontal made by routines based on
SLALIB functions

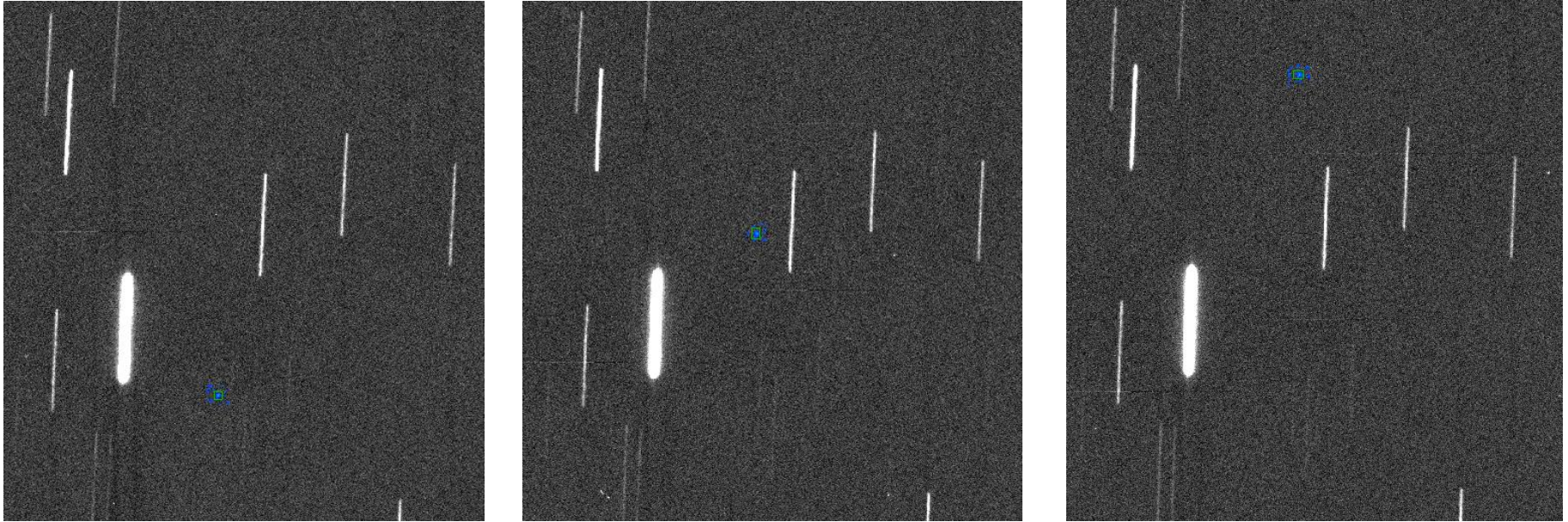
Standardized atmosphere parameters are
used

Plate model parameters are calculated
using least-square fitting method with
several iterations

The initial astrometric reduction of CCD frames with stars is standard and made by ***Astrometrica*** software with *Gaia* DR2 star catalogue as reference system.

Rotating drift-scan CCD approach

Processing and astrometric reductions



NEOCP object observed on 2021-09.12. Provisional designation - C28NMZ1 (2021 RJ₁₄)

Determination of target object's rectangular coordinates is made by weighted average method:

$$X_0 = \frac{\sum_{i=i1}^{i2} \sum_{j=j1}^{j2} X_{ij} I_{ij}}{\sum_{i=i1}^{i2} \sum_{j=j1}^{j2} I_{ij}} \quad Y_0 = \frac{\sum_{i=i1}^{i2} \sum_{j=j1}^{j2} Y_{ij} I_{ij}}{\sum_{i=i1}^{i2} \sum_{j=j1}^{j2} I_{ij}}$$

Telescopes

RI "MAO"

Mykolaiv, Ukraine

MPC observatory code 089



Telescope: D = 500 mm
F = 2975 mm

Time accuracy: GPS, rounded to
0.001s

CCD camera: CCD Alta U9000

Active Pixels 3k x 3k

Pixel Size 12 x 12 μm^2

FOV 42.5' x 42.5'

Scale: 0.83" x 0.83"/px

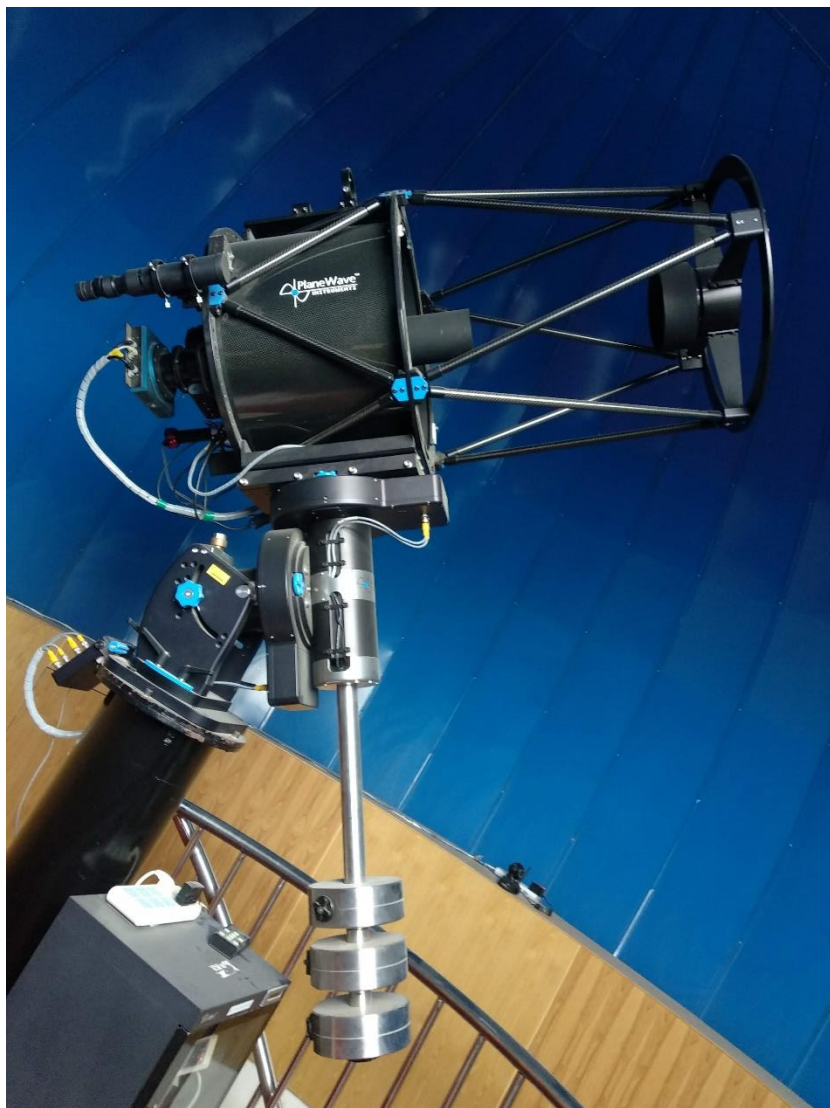
Photometric system: since 2018 - standard V, R filters
(Johnson-[Cousins UBVRI photometric system](#))

Telescopes

LiShan observatory

Lintong, Xi'An, China

MPC observatory code O85



Telescope: D = 500 mm
F = 3445 mm

Time accuracy: GPS, rounded to
0.001s

CCD camera: CCD Alta U9000

Active Pixels 3k x 3k

Pixel Size 12 x 12 μm^2

FOV 36.7' x 36.7'

Scale: 0.72" x 0.72"/px

Features:

- Half automatic and remotely controlled;
- No filters for now

Observational program

The objects for observations are searched on the daily basis at:

1) NEAs (PHA with medium priority) via NEODyS-2 query form:

<https://newton.spacedys.com/neodys/>

additional criteria: ap. rate of motion $\geq 0.15''/s$ (according to FWHM)

(automatically)

2) Objects from NEO Confirmation Page lists (higher priority):

<https://newton.spacedys.com/neodys/NEOScan/>

<https://cneos.jpl.nasa.gov/scout/#/>

(automatically)

3) Objects from the Priority List (higher priority):

<https://neo.ssa.esa.int/priority-list>

(manually)

Selection criteria:

ap. magnitude ≤ 18 mag;

declination $> -25^\circ$ (for O89); $> -45^\circ$ (for O85);

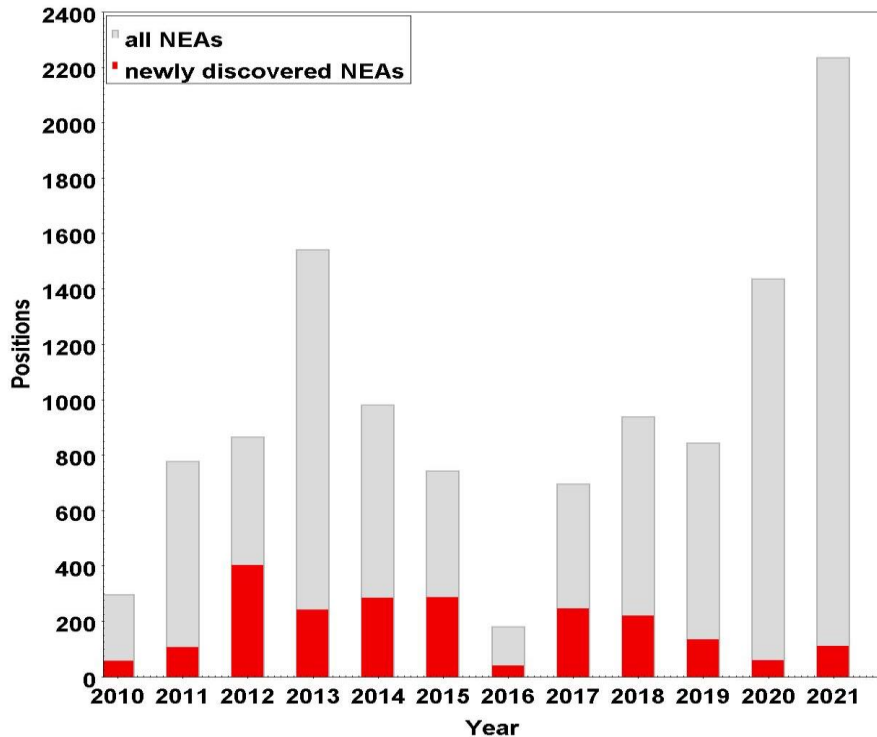
elongation $\geq 85^\circ$;

Astrometry results

Obtained observational data array

089 - RI “MAO”

Total number of NEAs obtained positions is more than **13,000** for 540 NEAs during 2010 -2021.



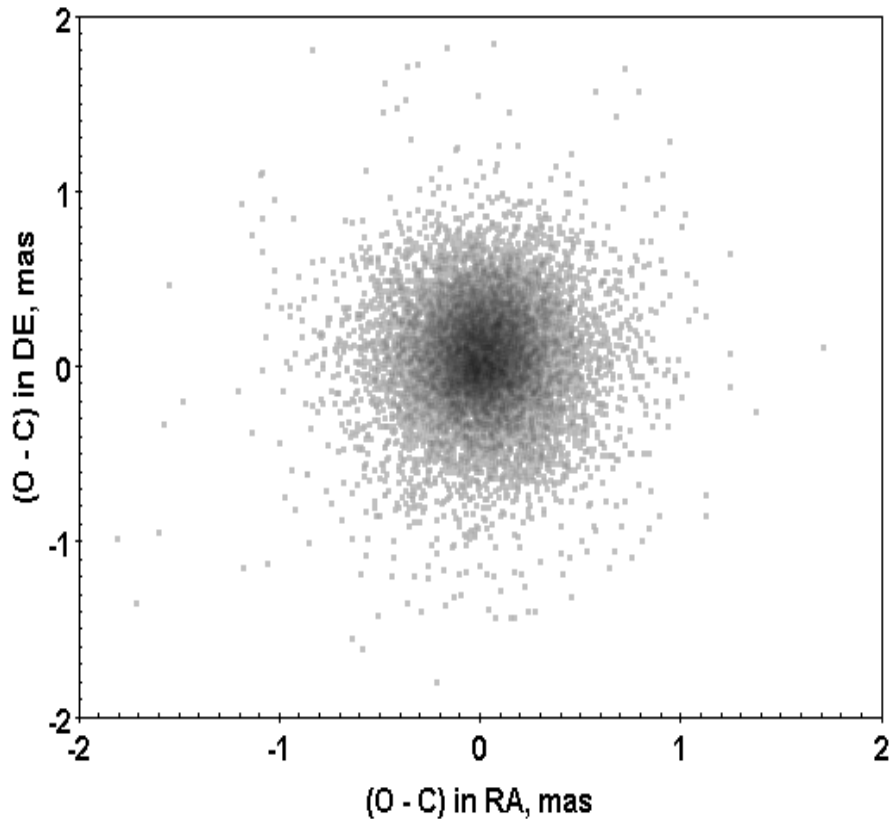
085 - LiShan Observatory

Total number of obtained positions is **1616** for **92** NEAs. Among them **352** positions for **24** newly discovered ones.

Year	N1	N2	Newly discovered	
			n1	n2
2019	368	16	54	2
2020	462	34	32	3
2021	786	43	266	19

Astrometry results

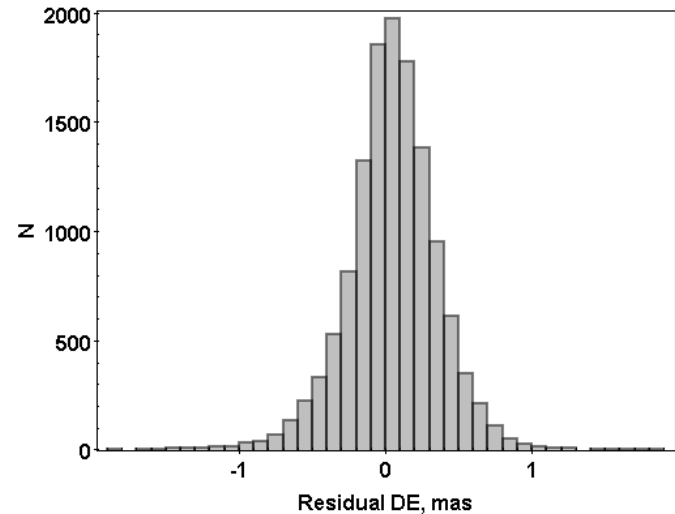
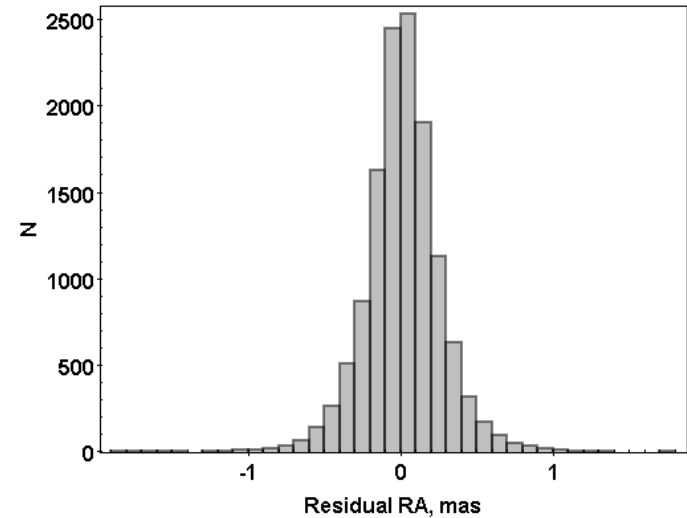
Astrometric accuracy and analysis. RI “MAO” (089)



$(O - C) \text{ in RA} = (0.01 \pm 0.24)''$

$(O - C) \text{ in DEC} = (0.05 \pm 0.30)''$

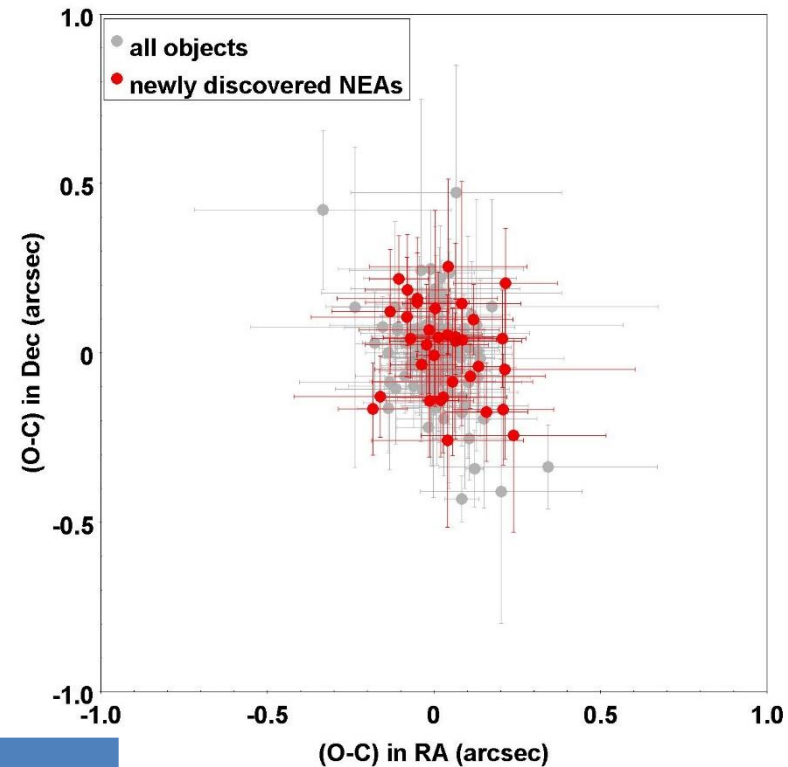
Only 2% residuals exceed the value $1''$



Astrometry results

Astrometric accuracy and analysis. LiShan observatory (O85)

The precision for both newly discovered and already known NEAs is in the range $0.1'' - 0.2''$ in both coordinates. However, the mean apparent rate of motion among known objects is $10.4'' \text{ min}^{-1}$ while is $43.7'' \text{ min}^{-1}$ for newly discovered NEAs.



Year	$(O - C) \pm \sigma (")$			
	Already known NEAs		Newly discovered NEAs	
	RA	Dec	RA	Dec
2019	-0.01 ± 0.09	0.04 ± 0.11	-0.04 ± 0.13	0.16 ± 0.20
2020	-0.02 ± 0.13	-0.01 ± 0.16	0.01 ± 0.13	-0.05 ± 0.16
2021*	0.01 ± 0.14	-0.04 ± 0.14	0.05 ± 0.17	0.00 ± 0.17

Astrometry results

Results for newly discovered NEAs (code 089)

NEO	N1	N2	Uncert. Param.	App. Motion, * "/min		(O - C) ± σ, "		Mag
				max.	mean obs.	RA	Dec	
K20Q06V	160	19	6	67.8	31.6	-0.01 ± 0.13	0.37 ± 0.17	16.4
K20R00C	275	10	5	41.6	36.1	-0.03 ± 0.13	0.21 ± 0.15	15.9
K20R06Z	89	9	5	315.9	234.2	-0.16 ± 0.27	0.16 ± 0.18	16.4
K20S00W	149	8	5	3414.6	32.4	0.14 ± 0.08	0.42 ± 0.14	16.0
K20R00J	108	7	4	91.1	88.9	-0.75 ± 0.30	0.38 ± 0.22	16.6
K20P04T	38	4	6	82.1	41.0	0.02 ± 0.29	-0.34 ± 0.26	16.9
K20N01K	114	3	6	46.3	25.1	0.05 ± 0.14	-0.05 ± 0.09	15.9
K21J01G	162	10	5	134.2	97.9	0.13 ± 0.14	0.17 ± 0.17	15.5
K21N04M	64	10	6	102.4	102.2	0.02 ± 0.23	0.16 ± 0.33	16.1
K21K00C	97	7	7	32.3	27.4	-0.05 ± 0.26	0.49 ± 0.26	17.0

* The column **max.** shows maximum apparent motion with respect to Geocenter; the column mean **obs.** – regarding observational site (code O85)

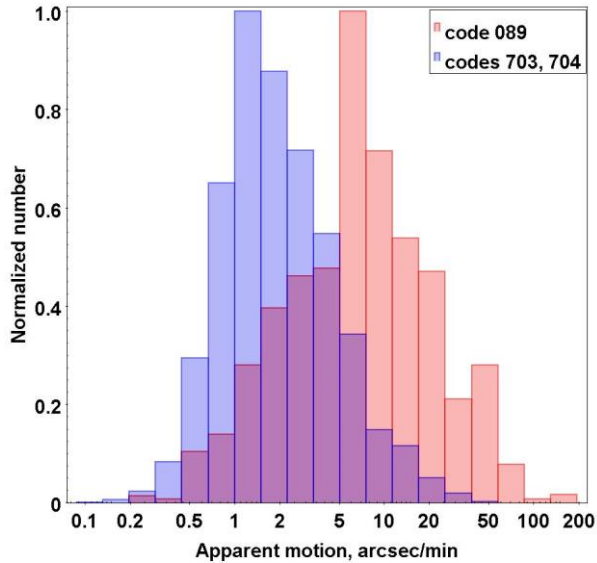
Astrometry results

Results for newly discovered NEAs (code O85)

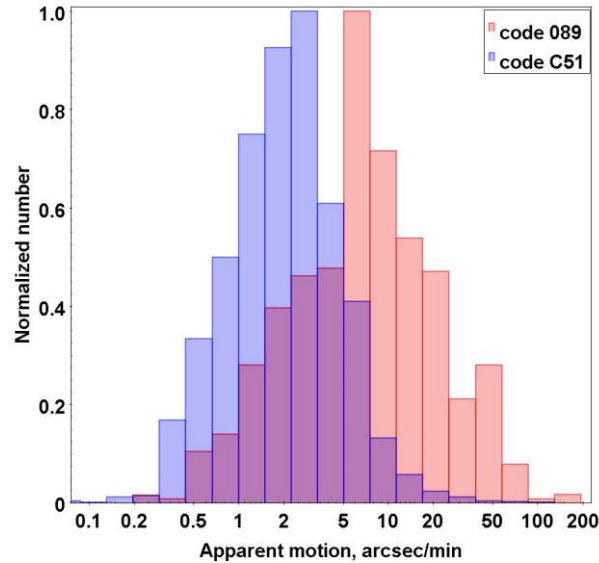
NEO	N1	N2	Uncert. Param.	App. Motion, * "/min		(O - C) ± σ, "		Mag
				max.	mean obs.	RA	Dec	
K20W05U	66	156	2	32.8	24.0	0.04 ± 0.11	0.04 ± 0.12	13.8
K21C00O	16	86	6	389.9	218.5	0.37 ± 0.15	0.28 ± 0.13	14.0
K21C02K	29	193	3	19.0	11.9	-0.05 ± 0.15	0.03 ± 0.15	15.9
K20C01X	16	153	0	42.6	42.3	0.03 ± 0.14	-0.19 ± 0.17	17.6
K20M03X	11	142	4	25.2	25.2	0.02 ± 0.05	-0.13 ± 0.17	16.3
K21C06A	22	44	3	359.2	336.4	-2.03 ± 0.25	-0.05 ± 0.18	17.4
K21D01W	14	269	3	82.5	82.2	-0.14 ± 0.10	-0.18 ± 0.14	14.4
K21F00H	10	92	7	26.3	25.6	-0.01 ± 0.13	-0.14 ± 0.17	17.0
K21F01K	15	49	7	54.8	53.4	0.24 ± 0.28	-0.24 ± 0.29	17.4
K21V02R	9	59	6	177.8	80.8	-0.52 ± 0.23	0.13 ± 0.26	17.4

* The column **max.** shows maximum apparent motion with respect to Geocenter; the column mean **obs.** – regarding observational site (code O85)

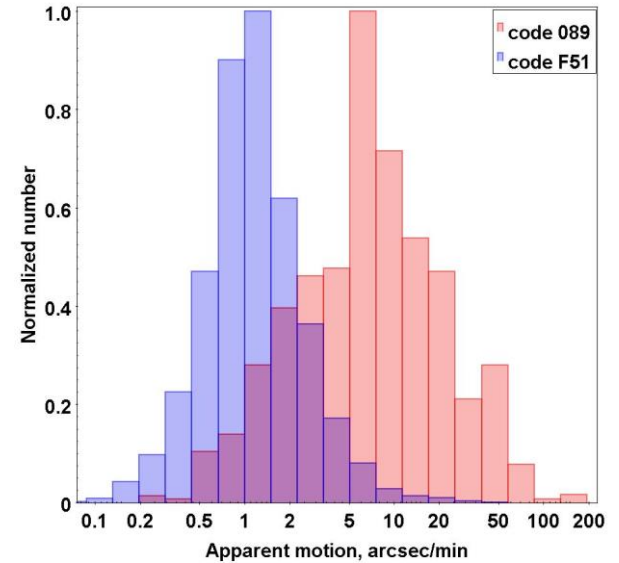
Astrometry results



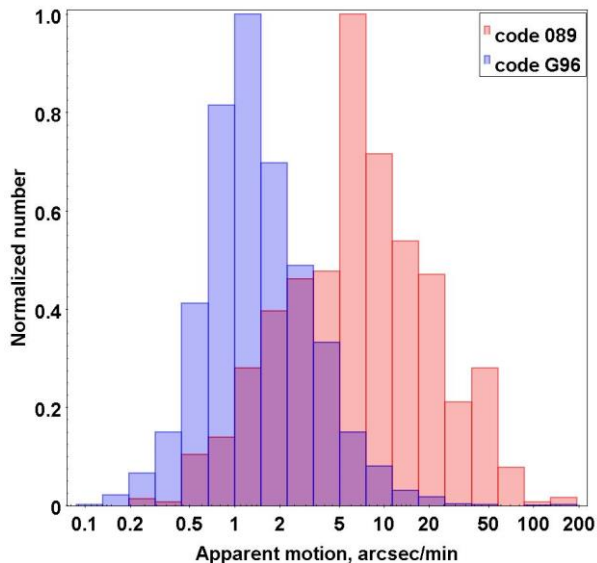
a) $2.98''/\text{min} \pm 3.67''/\text{min}$



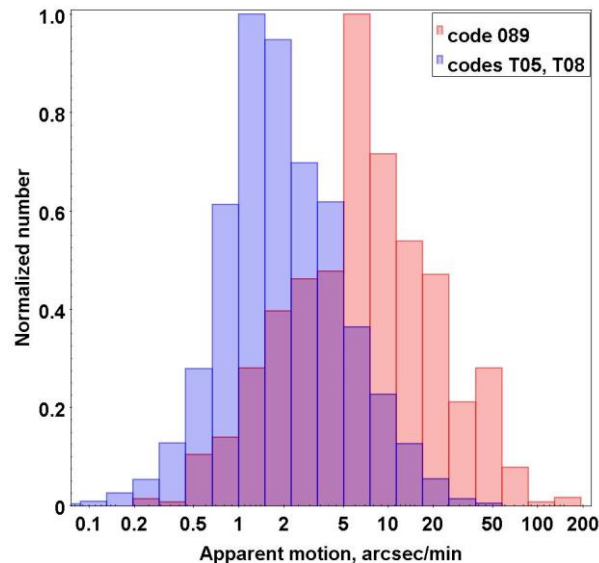
b) $2.85''/\text{min} \pm 3.49''/\text{min}$



c) $1.59''/\text{min} \pm 2.04''/\text{min}$



d) $2.26''/\text{min} \pm 8.40''/\text{min}$



e) $3.10''/\text{min} \pm 3.89''/\text{min}$

The distribution of apparent rate of motion for NEAs' observations since 2010 for selected observatories/surveys in comparison to observations of 089 ($11.84''/\text{min} \pm 14.94''/\text{min}$)

Astrometry results

Analysis of observations (2017 YE5)

The asteroid was discovered at December 2017.

Only 95 observations were available within 191d orbital arc.

Close approach to Earth to 0.04 AU was at **Jun 22, 2018**.

Date 2018	O-C, ''		Date 2018	O-C, ''	
	RA	Dec		RA	Dec
06-20.966624	-10.669	-7.228	06-20.966624	-0.137	0.005
06-20.971275	-10.567	-7.067	06-20.971275	-0.040	0.174
06-20.977173	-10.325	-7.516	06-20.977173	0.196	-0.264
06-20.981830	-10.430	-6.835	06-20.981830	0.087	0.426
06-20.987260	-10.290	-6.990	06-20.987260	0.221	0.281
06-20.989585	-10.307	-7.638	06-20.989585	0.202	-0.363
mean (O-C)	10.431	-7.212	mean (O-C)	0.088	0.043
σ	0.156	0.312	σ	0.148	0.310

Arecibo/GBO/JPL/NASA/NSF

2017 YE5

2018 Jun 25 UT

(O-C) differences **before** and **after** adding own observations

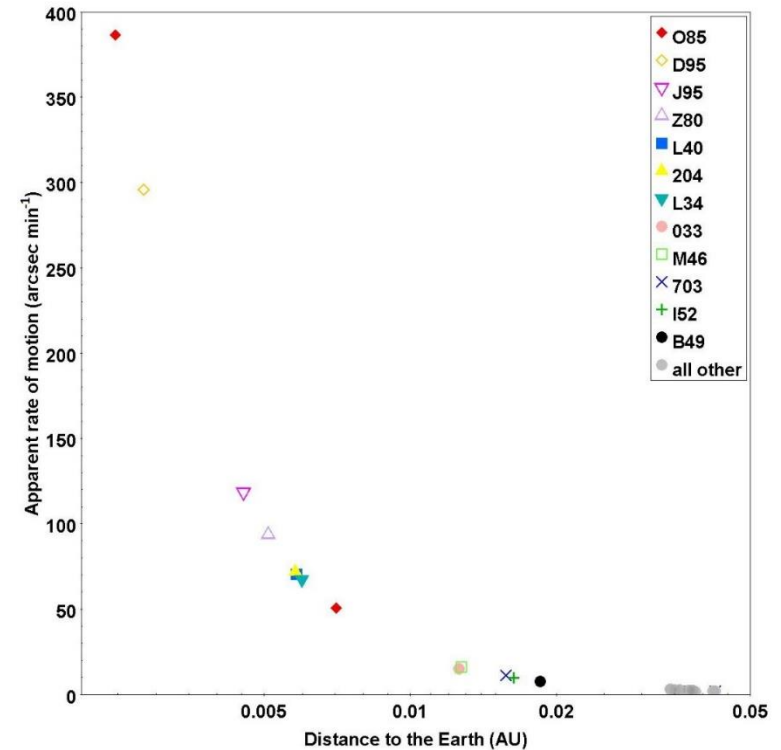
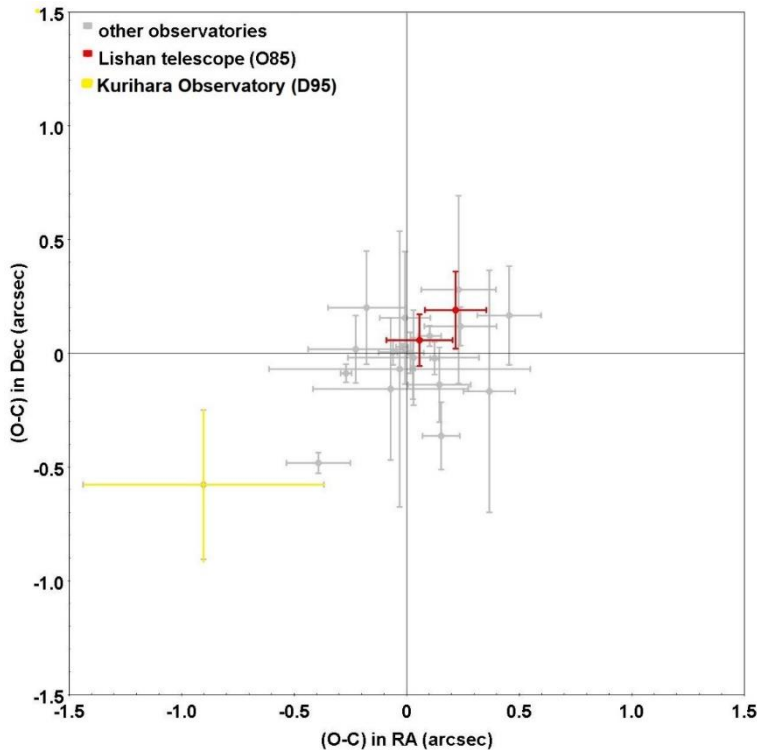
Astrometry results

Analysis of observations (2021 CO)

The asteroid was discovered on
Feb 5, 2021.

	Initial calc.		Final calc.	
	RA	Dec	RA	Dec
mean	0.63	0.50	0.22	0.19
σ	0.16	0.16	0.14	0.17

Only 99 positions available over 6d



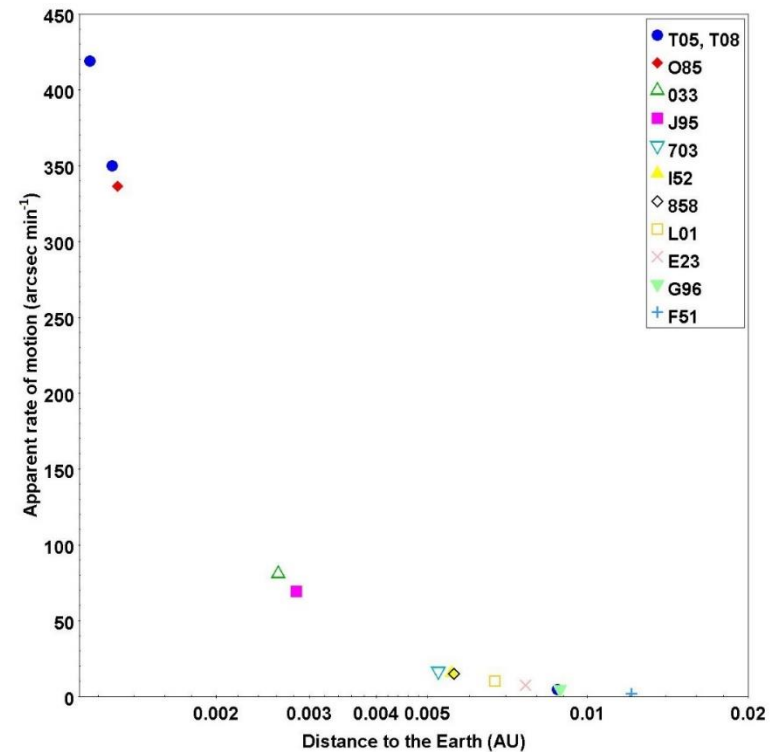
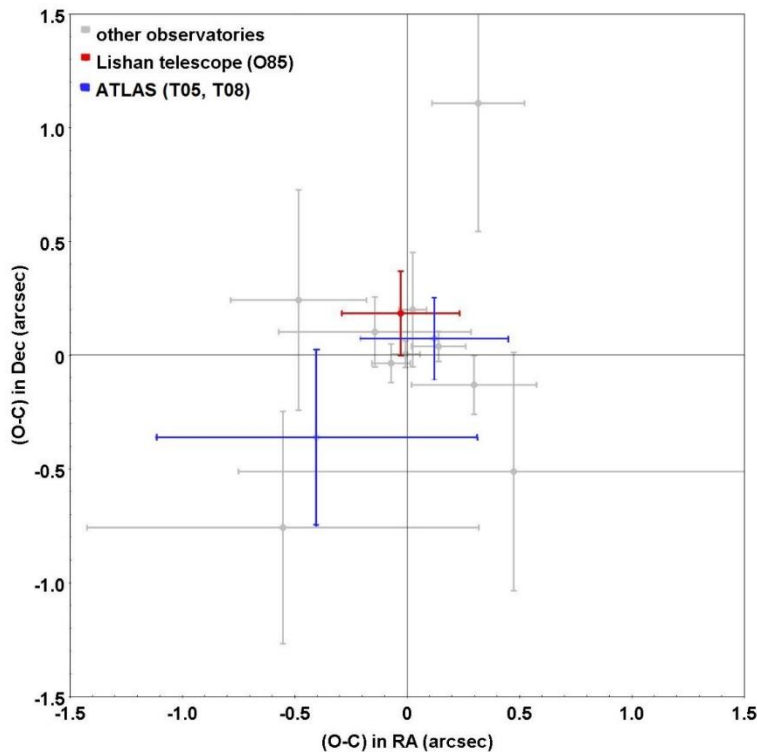
Astrometry results

Analysis of observations (2021 CA6)

The asteroid was discovered on
Feb 10, 2021.

	Initial calc.		Final calc.	
	RA	Dec	RA	Dec
mean	-2.03	-0.05	-0.03	0.18
σ	0.25	0.18	0.26	0.19

Only 66 positions available over 3d



Astrometry results

Orbital analysis

Calculations were done in 2 ways:

- all positions used (all)
- positions without CA date (w/o CA)

NEA		N obs.	rms (")	a (au)	e	i (°)	n (°/day)	Ω (°)	ω (°)	MA (°)	CA date	σ (")
K20N01K	all	119	0.29	1.30E-03	3.10E-04	2.10E-02	8.50E-04	1.60E-03	2.70E-02	6.00E-02	04-08-2043	1643
	w/o CA	108	0.27	1.50E-03	3.60E-04	2.50E-02	9.80E-04	1.90E-03	3.20E-02	7.00E-02		173d
K21C000	all	60	0.24	1.50E-04	1.70E-04	2.30E-03	1.60E-04	4.80E-05	4.40E-04	2.70E-02	27-08-2022	917
	w/o CA	43	0.24	4.00E-04	5.30E-04	6.00E-03	4.50E-04	4.80E-03	6.00E-03	8.00E-02		2585
K21U09M	all	200	0.41	8.00E-04	1.40E-04	4.80E-04	1.40E-04	2.80E-04	6.00E-04	4.60E-03	08-02-2029	406'
	w/o CA	178	0.42	1.00E-03	1.80E-04	6.00E-04	1.80E-04	3.60E-04	7.00E-04	5.90E-03		936'
K21V02R	all	87	0.6	1.40E-03	2.20E-04	1.80E-03	2.10E-04	1.30E-05	8.00E-05	3.70E-03	26-11-2085	664'
	w/o CA	66	0.48	2.10E-03	3.10E-04	2.60E-03	2.90E-04	2.20E-05	1.60E-04	5.40E-03		62d

Orbit determination shows reducing of sky uncertainty with adding new positions near CA date and extending orbital arc

Conclusions

- A large telescope without secured follow-up is inefficient at turning its NEA candidates into NEAs discoveries!!!
- The using RDS CCD technique for NEAs observations allows us to observe the objects on minimal distances to the Earth with high apparent rate of motion with a good accuracy.
- The RDS CCD technique allows to extend observed orbital arc with high-precision positions around CA date. Such results are essentially important for newly discovered NEAs, allow to improve orbit determination and make reliable assessment, prevent object losses.
- Worldwide network of small telescopes with RDS CCDs would have strong advantages to observe all NEAs especially PHAs for better astrometry and photometry.
- SHAO and RI “MAO” would like to cooperate to any observatory with the same interests and provide technical support.

Thank you!